Published in final edited form as:
Biochemistry. 2008 March 25; 47(12): 3917–3925. doi:10.1021/bi702530z.

Oxidative Metabolism of a Fatty Acid Amide Hydrolase-Regulated Lipid, Arachidonoyltaurine†

Melissa V. Turman‡, **Philip J. Kingsley**‡, **Carol A. Rouzer**‡, **Benjamin F. Cravatt**§, and **Lawrence J. Marnett**‡,*

‡A. B. Hancock, Jr. Memorial Laboratory for Cancer Research, Departments of Biochemistry, Chemistry, and Pharmacology, Vanderbilt Institute of Chemical Biology, and Center in Molecular Toxicology, Vanderbilt University School of Medicine, Nashville, Tennessee 37232 USA

§The Skaggs Institute for Chemical Biology, Departments of Cell Biology and Chemistry, The Scripps Research Institute, La Jolla, California 92037 USA

Abstract

A novel class of lipids, *N*-acyltaurines, was recently discovered in fatty acid amide hydrolase knockout mice. In some peripheral tissues, such as liver and kidney, *N*-acyltaurines with long, polyunsaturated acyl chains are most prevalent. Polyunsaturated fatty acids are converted to a variety of signaling molecules by cyclooxygenases (COXs) and lipoxygenases (LOXs). The ability of COXs and LOXs to oxygenate arachidonoyltaurine was evaluated to gain insight into the potential metabolic fate of *N*-acyltaurines. Although arachidonoyltaurine was a poor substrate for COXs, mammalian 12*S*- and 15*S*-LOXs oxygenated arachidonoyltaurine with similar or better efficiency than arachidonic acid. Products of arachidonoyltaurine oxygenation were characterized by LC-MS/MS. The positional specificity of single oxygenation was retained for 15*S*-LOXs. However, platelet-type 12*S*-LOX produced 12- and 15-hydroxyeicosatetraenoyltaurines (HETE-T). Furthermore, LOXs generated dihydroxyeicosatetraenoyltaurines (diHETE-T). Metabolism of arachidonoyltaurine by murine resident peritoneal macrophages (RPMs) was also profiled. Arachidonoyltaurine was rapidly taken up and converted primarily to 12-HETE-T. Over prolonged incubations, RPMs also generated small amounts of diHETE-T. Oxidative metabolism of polyunsaturated *N*-acyltaurines may represent a pathway for the generation or termination of novel signaling molecules.

The endocannabinoid system has emerged as a critical therapeutic target in recent years (1). Numerous pathophysiological conditions including mood disorders, osteoporosis, myocardial ischemia/reperfusion injury, and cancer could potentially be treated by modulation of the endocannabinoid system (1-8). One approach to the manipulation of this system is the inhibition of fatty acid amide hydrolase (FAAH)[1] (9). FAAH has a central role in the regulation of fatty acid amide levels *in vivo*, including those of the endocannabinoid arachidonoylethanolamide (AEA, Fig. 1). Discovery metabolite profiling has revealed that another, previously unidentified class of lipids, *N*-acyltaurines (NATs), are substantially increased by chemical or genetic knockout of FAAH (10,11). NATs are able to activate members of the transient receptor potential family of calcium ion channels in a cellular system (10). With the exception of these reports, the signaling and catabolic pathways for *NATs* have not been elucidated.

†This work was supported by National Institutes of Health Research Grant CA89450 (L.J.M.) and a training grant to M.V.T. (ES07028). M.V.T is the recipient of a Ruth L. Kirschstein National Research Service Award (DA02014) from the National Institutes of Health/ National Institute of Drug Abuse and a fellowship from the Vanderbilt Institute of Chemical Biology.

*CORRESPONDING AUTHOR. Department of Biochemistry, Vanderbilt University School of Medicine, Nashville, Tennessee 37232-0146. Phone: 615-343-7329. Fax: 615-343-7534. larry.marnett@vanderbilt.edu..

An initial approach to determine potential metabolic pathways is to probe the interactions of a novel molecule against enzymes that are known to metabolize related species. In peripheral tissues, such as liver and kidney, NATs possessing long, polyunsaturated acyl chains are most prevalent (10). Linoleoyl (18:2), arachidonoyl (20:4), and docosahexaenoyl (22:6) taurines were increased from twenty-to more than one hundred-fold in the livers of FAAH knockout mice. The parent polyunsaturated fatty acids are susceptible to both enzymatic and non-enzymatic peroxidation of the allylic chain, and this process plays a central role in the biology and pathophysiology of lipid signaling. Prostaglandins (PGs) and hydroxyeicosatetraenoic acid (HETEs) are generated from the oxygenation of arachidonic acid by cyclooxygenase (COXs) and lipoxygenases (LOXs), respectively, and serve as critical local bioactive mediators of cellular signaling (12-14). Moreover, these enzymes have been implicated in the metabolism of arachidonoyl derivatives, including the endocannabinoids 2-arachidonoylglycerol (2-AG) and AEA (Fig. 1) (15).

COX-1 and COX-2 are homologous proteins, differing primarily in their expression profiles and, consequently, their physiological and pathophysiological functions (13,16). Both isoforms exhibit similar kinetics and product profiles with arachidonic acid (16,17). However, the volume of the COX-2 active site is approximately 20% larger than that of COX-1 (18). As a result, the COX-2 active site is able to accommodate a variety of esters and amides of arachidonate, including 2-AG and AEA, as well as arachidonoyl amino acids such as *N*-arachidonoylglycine (NAGly) (19-24). In contrast, COX-1 uses these substrates inefficiently, if at all.

Multiple isoforms of LOXs have been cloned from mammals and are classified by the position and stereochemistry of oxygen addition to arachidonic acid (25). Although all LOXs catalyze a single dioxygenation of polyunsaturated fatty acids, the regio- and stereospecificity of oxygenation varies between isoforms, as does substrate specificity. 15*S*-LOX-1 and leukocyte-type 12*S*-LOX (lk12-LOX) are promiscuous enzymes, metabolizing a range of C_{18}, C_{20}, and C_{22} fatty acids (26-28). These isoforms will also oxygenate fatty acid amides and esters such as 2-AG, AEA, and NAGly (23,29-32). 15*S*-LOX-1 and lk12-LOX can even incorporate oxygen into polyunsaturated acyl chains of phospholipids (33,34). In contrast, platelet-type 12*S*-LOX (pl12-LOX) shows a marked preference for C_{20} fatty acids and is unable to efficiently metabolize neutral amides and esters of arachidonate (26,29,30,32,34-36). Notably the lipoamino acids NAGly, *N*-arachidonoylalanine (NAla), and *N*-arachidonoyl-γ-aminobutyric acid (NAGABA), which would bear a negative charge at physiological pH, are kinetically comparable to arachidonic acid; however, the positional specificity of pl12-LOX is altered, and the enzyme acts as a 12/15-LOX on these substrates (23). Human 15*S*-LOX-2 also utilizes the arachidonoyl amino acids efficiently but maintains its positional specificity.

The COX and LOX pathways may modify polyunsaturated NATs and thus alter the activity of NATs *in vivo*. We investigated the ability of these enzymes to metabolize arachidonoyltaurine. We demonstrate that 15-LOX-1, lk12-LOX and pl12-LOX, but not COX, can catalyze the peroxidation of arachidonoyltaurine, though with some perturbations of typical product profiles. We further characterized the ability of murine resident peritoneal macrophages to metabolize arachidonoyltaurine and show that arachidonoyltaurine is able to enter the LOX pathway in cells. LOX metabolism of arachidonoyltaurine may represent a pathway of termination or biosynthesis of signaling molecules.

Materials and Methods

Reagents

Arachidonic acid and arachidonoylchloride were purchased from NuChek Prep (Elysian, MN). Arachidonoyltaurine was purchased from Cayman Chemical (Ann Arbor, MI). Ram seminal

vesicles were purchased from Oxford Biomedical Research (Oxford, MI), and oCOX-1 was purified as previously described (37). Expression of mCOX-2 was performed with baculovirus reagents from BD Biosciences (San Diego, CA). Human 15-LOX-2 (h15-LOX-2) was expressed in bacteria. Purification procedures for mCOX-2, h15-LOX-2, and human platelet 12-LOX (pl12-LOX) were described previously (22,31,38). All of the expressed proteins were over 95% pure by SDS-PAGE staining and analysis, except for h15-LOX-2, which was 70% pure. Cell lysates containing rabbit reticulocyte 15-LOX-1 (r15-LOX-1) were purchased from Calbiochem (La Jolla, CA), and porcine leukocyte 12-LOX (lk12-LOX) was purchased from Cayman Chemical (Ann Arbor, MI).

COX Activity Assay

Quantification of cyclooxygenase activity was performed in a thermostatted cuvette at 37° C and monitored using a polarographic electrode with a YS5300 oxygen monitor (Yellow Springs Instrument Co. Inc., Yellow Springs, OH). Substrates were solubilized in dimethyl sulfoxide (DMSO). Activity assays were performed in 100 mM Tris-HCl buffer containing 500 μM phenol, with hematin-reconstituted protein (50 nM). Maximal reaction velocity data were obtained from the linear portion of the oxygen uptake curves and normalized to the metabolism rate of arachidonic acid.

LOX Activity Assay

LOX activity was detected by monitoring the absorbance of the conjugated diene product at 236 nm. UV assays were monitored using a Hewlett Packard 8453 diode array spectrophotometer equipped with a thermostatted cuvette at 25° C, with stirring at 180 RPMs. The enzyme reactions included reaction buffer [50 mM Tris-HCl (pH 7.4) with 0.03% Tween-20] and substrate, and were initiated by the addition of enzyme (r15-LOX-1 - 3.7 μg/ml, h15-LOX-2 - 170 μg/ml, lk12-LOX - 200 μg/ml and pl12-LOX - 2 μg/ml). Compounds were dissolved in acetonitrile (ACN) containing 10 % acetic acid before addition to the reaction buffer; ACN was kept below 1% reaction volume (2 ml). For the initial metabolism screen, compounds were diluted to a final concentration of 25 μM. To determine Michaelis-Menten kinetic parameters the concentration of substrate was varied (1-50 μM). Maximal reaction velocity data were obtained from the linear portion of the absorbance curves, and the data were analyzed by nonlinear regression with Prism 4.0 (GraphPad Software, San Diego, CA).

Enzyme incubations for product identification

To characterize products of oxidation, 5 μg enzyme was incubated with 50 μM arachidonoyltaurine in 50 mM Tris-HCl, pH 8.0. After allowing the reaction to proceed for 15 min, one volume 1 M sodium thiosulfate was added to reduce hydroperoxides to corresponding alcohols. The reaction mixture was then extracted with 3 volumes ethyl acetate containing 0.5% acetic acid and 1 μM arachidonic acid-d_8. The organic layer was removed and dried under argon, and the resulting residue stored at -20°C until analysis. For LC-MS analysis, the residue was resuspended in 1:1 methanol/5 mM ammonium acetate (pH 6.9) and passed through a SpinX filter to remove precipitate.

RPMs cultures

These experiments were done with the approval of the Vanderbilt IACUC. Female CD-1 mice (25–30 g) were obtained from Charles River Laboratories (Wilmington, MA). The mice were sacrificed by asphyxiation with carbon dioxide, and the peritoneal cavities were lavaged with a total of 3 ml of ice-cold calcium- and magnesium-free phosphate-buffered saline (PBS) (39). Peritoneal cells were collected by centrifugation of lavage fluid and resuspended at a concentration of 2–3 × 10^6 cells/ml in α-minimal essential medium (α-MEM) supplemented with GlutaMAX (Invitrogen) containing 10% heat-inactivated fetal calf serum (FCS; Summit

Biotechnologies, Fort Collins, CO) plus 100 units/ml penicillin and 0.10 mg/ml streptomycin (Sigma) (α-MEM/FCS). The cell suspension was plated onto 35-mm tissue culture dishes at 2 ml/dish or onto 60-mm dishes at 6 ml/dish and incubated for 2 h at 37 °C in a humidified 5% CO_2 atmosphere. Nonadherent cells were removed by washing the plates four times with PBS, and the cultures were then incubated overnight in fresh α-MEM/FCS. The mean protein content of RPMs cultures (35-mm dish) was 100 ± 10 μg/dish ((8.2 ± 0.8) × 10^5 cells/dish). Cultures of RPMs were washed twice with PBS at 37 °C and then overlaid with 1 ml of fresh α-MEM containing 25 μM arachidonic acid or arachidonoyltaurine. Cells were incubated with 25 μM arachidonic acid or arachidonoyltaurine for either 30 s or 15 min. The medium was removed and extracted with 3 volumes of ethyl acetate containing 0.5% acetic acid and 1 μM arachidonic acid-d_8. Extracts were dried under argon and resuspended in 1:1 methanol/5 mM ammonium acetate (pH 6.9).

LOX product characterization

LC was conducted on a a Surveyor Separation Module using a Luna C18(2) column (50 × 2 mm, 3 μm) equipped with a C18 (2) Security Guard. The mobile phase consisted of 5 mM ammonium acetate, pH 6.9 (solvent A) and 3% A in acetonitrile (solvent B), and flow was constant at 0.3 ml/min. Gradient increased from 30% B to 90% B over 5 minutes, followed by a hold at 90% B for 4 minutes. Flow from the column passed first through a UV detector set to monitor 236 nm before proceeding to the electrospray ionization source. MS and MS/MS were conducted on a Quantum Triple Quadrupole Mass Spectrometer. The instrument was operated in negative ion mode using electrospray ionization with a spray voltage of 4.5 kV and capillary temperature of 225°C. Full scan analysis was performed from 295 to 500 *m/z* with a scan time of 1.2 s. Peaks of interest were selected for CID and fragmented in Q2. The collision energies used were: -35 eV for *m/z* 442, -40 eV for *m/z* 426, -15 eV for *m/z* 335, and -25 eV for *m/z* 319. The mass range for detection in Q3 was set to 75 to 450 *m/z*.

Protein expression and immunoblotting

Following removal of the medium from RPMs for product characterization, cells were scraped twice into 100 μl lysis buffer (50 mM Tris-HCl, pH 7.5, plus 150 mM NaCl, 4 mM EDTA, 50 mM NaF, 0.1 mM Na_3VO_4, 0.2% Triton X-100, 0.1% NP40, 0.5% sodium deoxycholate, 1 mg/ml 4-(2-aminoethyl)benzenesulfonyl fluoride, and 5 μg/ml each of antipain, leupeptin, chymostatin, and pepstatin) and stored at -80°C. Protein concentrations were determined using Bradford protein assay (Bio-Rad, Hercules, CA). Either 5 or 10 μg of protein from RPMs and lysis buffer (as control) were subjected to SDS-polyacrylamide gel electophoresis. Proteins were then transferred to nitrocellulose membrane (0.2 μm), which was treated with Miser Antibody Extender Solution (Pierce, Rockford, IL) prior to blocking with 5% non-fat milk protein in 20 mM Tris-HCl and 100 mM NaCl (pH 7.5) containing 0.1% Tween-20 (TTBS). 12/15-LOX was detected following incubation with a rabbit polyclonal antiserum directed against purified murine recombinant leukocyte 12-LOX (Cayman Chemical, Ann Arbor, MI) diluted 1:3000 in TTBS with 0.1% milk protein; it should be noted that this antibody cross reacts with pl12-LOX and r15-LOX-1 from other species. FAAH was detected following incubation with a rabbit polyclonal antibody directed against a synthetic peptide of rat FAAH amino acids 561-579 conjugated to KLH (Cayman Chemical, Ann Arbor, MI) diluted 1:1000 in TTBS with 0.1% milk protein. The secondary antibody used for both blots was horseradish peroxidase-conjugated anti-rabbit IgG (GE Healthcare, Piscataway, NJ), diluted 1:4000 in TTBS with 0.1% milk protein. After the membranes were overlaid with ECL detection reagents (GE Healthcare, Piscataway, NJ), the membranes were exposed to Hyperfilm ECL (GE Healthcare, Piscataway, NJ) to obtain photographic images.

Results

Oxygenation of arachidonoyltaurine by COXs and LOXs

COX-2 and several LOXs are able to metabolize a variety of arachidonoyl containing substrates, including AEA, 2-AG, and NAGly (15,22,23). Given the structural similarity of these substrates, the ability of COXs and LOXs to metabolize arachidonoyltaurine was investigated. At a concentration of 25 μM, arachidonoyltaurine was a very poor substrate for COX-1 and COX-2, with oxygenation proceeding at a rate of less than 10% of that observed for arachidonic acid. In contrast, r15-LOX-1, pl12-LOX, and lk12-LOX efficiently metabolized arachidonoyltaurine.

The kinetics of arachidonoyltaurine oxygenation by r15-LOX-1, pl12-LOX, and lk12-LOX were determined by monitoring formation of the conjugated diene system via absorbance at 236 nm. In some cases, the concentration-dependence of rates could not be fit to the classical Michaelis-Menten equation, and the concentration-dependence was fit by linear regression. The concentration range for regression was selected such that R^2 was greater than 0.9, and v_{max}/K_M was estimated from the slope of this line (Table 1). As judged by v_{max}/K_M, the efficiency of arachidonoyltaurine metabolism was similar to or better than that of arachidonic acid for all LOX isoforms examined. In contrast to r15-LOX-1 and lk12-LOX, pl12-LOX exhibited apparent substrate inhibition at high concentrations of arachidonoyltaurine (Fig. 2). Inhibition was at least partially abrogated by inclusion of low concentrations of 13-hydroperoxyoctadecadienoic acid (13-HpODE).

Characterization of products of arachidonoyltaurine oxygenation

Collisionally-induced dissociation (CID) of oxidized lipids can provide detailed structural information and is particularly useful for assigning regiochemistry of oxygenation (40,41). Lipid hydroperoxides are highly susceptible to in-source fragmentation resulting in the neutral loss of water. To reduce ambiguity resulting from in-source fragmentation, samples were treated with sodium dithionite to reduce hydroperoxides to the corresponding alcohols. The reduced products were subjected to analysis by LC-UV and tandem mass spectrometry (MS/MS). In addition, a standard of arachidonoyltaurine (*m/z* 410) was subjected to CID to establish fragment ions characteristic of the taurine moiety (Fig. 3). Such fragment ions were observed at *m/z* 80 (sulfonate), 107 (ethenesulfonate) and 124 (taurine). Additional fragment ions resulting from cleavage along the arachidonoyl chain were also observed. It was anticipated that the LOX reaction should not alter the taurine moiety or C-1 through C-4 of the acyl chain, and as such fragment ions at *m/z* 80, 107, 124, 151, 165, 178, and 192 should serve as a signature for the taurine moiety in LOX products.

Incubation of arachidonoyltaurine with r15-LOX-1 and h15-LOX-2 yielded similar product profiles, generating one major mono-oxygenated product (*m/z* 426) with retention time of 5.4 min and strong absorbance at 236 nm (Fig. 4 and 5A). CID of *m/z* 426 produced fragmentation patterns consistent with those reported for HETEs (40), but bearing characteristic fragment ions of the taurine moiety. In the case of r15-LOX-1 and h15-LOX-2, fragment ions with *m/z* 354 and 326 were observed (Fig. 5B). These ions are characteristic of fragmentation α to an alcohol at C-15.

12*S*-LOXs gave rise to quite different product profiles. pl12-LOX produced two distinct mono-oxygenated products with strong absorbance at 236 nm (Fig. 4). The product at 5.4 min fragmented to give CID spectra similar to that for 15-HETE-T (Fig. 5B). CID of the product at 5.6 min yielded a unique fragmentation pattern (Fig. 5C). In this case, fragment ions with *m/z* of 314 and 286 were characteristic of fragmentation α to the alcohol of 12-HETE-T. Thus the mass spectra suggested that the two major products were 15-HETE-T (~30%) and 12-

HETE-T (~70%). The elution order of the putative 15- and 12-HETE-T is consistent with that observed for arachidonic acid products 15- and 12-HETE (42). In contrast, lk12-LOX generated 12-HETE-T with no detectable 15-HETE-T.

In addition to HETE-T, LC-MS analysis revealed that each LOX produced one or two chromatographically distinct dioxygenated products with *m/z* of 442 (Fig. 6). These products appeared to account for less than 10% of the total products for r15-LOX-1, h15-LOX-2 and pl12-LOX. In contrast, diHETE-T accounted for almost 40% of total products formed by lk12-LOX. Positions of dioxygenation could not be definitively assigned by LC-MS/MS.

Oxidative metabolism of arachidonoyltaurine in resident peritoneal macrophages

RPMs provide a well-characterized system for the study of cellular uptake and metabolism of arachidonate-derived substrates. The profile of eicosanoid production, its modulation by various stimuli, and the expression of many arachidonate-metabolizing enzymes are well established in this system. RPMs were incubated with either arachidonic acid or arachidonoyltaurine for 30 s. Medium was removed and extracted, and extracts were analyzed by LC-UV-MS and MS/MS. As anticipated from *in vitro* studies, no prostanoids derived from arachidonoyltaurine were observed in incubations with RPMs. Within 30 s of incubation with arachidonoyltaurine, significant amounts of mono-oxygenated products were observed (Fig. 7A). Similar results were obtained with arachidonic acid (data not shown). All mono-oxygenated products absorbed strongly at 236 nm and yielded fragmentation patterns corresponding to HETE-derived species. In the case of arachidonic acid, the HETE isomers observed corresponded to oxygenation at C-5, C-12, or C-15. The major metabolite of arachidonoyltaurine was 12-HETE-T, though small amounts of 15-HETE-T were also observed. A 12/15-LOX was detected by immunoblotting. There was no evidence for oxygenation of arachidonoyltaurine at C-5.

Prolonged incubation of RPMs with arachidonic acid or arachidonoyltaurine afforded only modest increases (<20%) in mono-oxygenated products (Fig. 7B). However, a dioxygenated product was observed following incubation of RPMs with arachidonic acid or arachidonoyltaurine for 15 min. For arachidonic acid, the product with *m/z* 335 appeared to be oxygenated at C-5 and C-12. However, due to the low abundance of the diHETE-T product, which accounts for less than 5% of the total products of arachidonoyltaurine oxidation, definitive assignment of the positions of oxygenation could not be made. There was no evidence of hydrolysis of arachidonoyltaurine to arachidonic acid in RPMs after 15 min, and FAAH was not detectable by immunoblot.

Arachidonic acid metabolism in RPMS is altered by inflammatory stimuli; LPS increases prostanoid biosynthesis via induction of COX-2, and zymosan activates 5-LOX, resulting in increased synthesis of leukotrienes (43-50). To assess the effect of these stimuli upon arachidonoyltaurine metabolism, RPMS were preincubated with either LPS for six hours or zymosan for ten minutes. Cells were then washed and incubated with arachidonoyltaurine for 15 minutes, and the metabolic profiles were compared to those of unstimulated macrophages. Unlike arachidonic acid, arachidonoyltaurine metabolism was not affected significantly by LPS or zymosan (data not shown), suggesting that arachidonoyltaurine is not a good substrate for COX-2 or 5-LOX in cells.

Discussion

Inhibition of FAAH provides an attractive approach to modulating the endocannabinoid system, as it enhances the tonic actions of the endocannabinoids rather than indiscriminately activating all cannabinoid receptors. However, the recent discovery of NATs points to the

possibility of another effector molecule mediating some biological actions of FAAH inhibition. The pathways for the generation and degradation of NATs are only now being defined.

The current studies were aimed at investigating the interactions of a polyunsaturated NAT with important lipid metabolizing enzymes, COXs and LOXs. COX-2, but not COX-1, is able to metabolize a wide range of ester and amide derivatives of arachidonate (15,22,23). However, neither COX-1 nor COX-2 is able to utilize arachidonoyltaurine as a substrate. In contrast, 12*S*- and 15*S*-LOXs are able to oxygenate arachidonoyltaurine. In fact, pl12-LOX and r15-LOX-1 utilize arachidonoyltaurine more efficiently than arachidonic acid *in vitro*, and lk12-LOX exhibits similar efficiencies with arachidonate and arachidonoyltaurine.

Although arachidonoyltaurine is a very efficient substrate for pl12-LOX, the enzyme exhibited apparent substrate inhibition at high concentrations of arachidonoyltaurine. Although alkenyl sulfate substrates, including arachidonyl sulfate, are able to inhibit human 15-LOX-1, the mechanism of inhibition appears to be linked to aggregation of the substrate at high concentrations and can be eliminated by addition of detergent (51). This is likely not the cause of inhibition by arachidonoyltaurine, as detergent was included in the assay to prevent substrate aggregation. The phenomenon of substrate inhibition at high concentrations has been observed with LOXs and certain fatty acids. Perhaps the best-defined example is substrate inhibition in r15-LOX-1 and soybean 15-LOX-1 by linoleic acid (52-54). The rate-limiting step of the lipoxygenase reaction is the abstraction of a *bis*-allylic hydrogen from the substrate; this step can only be catalyzed by the ferric (Fe^{3+}) form of the enzyme (25). However, the resting enzyme exists in the ferrous (Fe^{2+}) form. The one-electron oxidation of the non-heme iron center by a hydroperoxide, such as 13-HpODE, activates the enzyme. Commercially supplied fatty acids and fatty acid derivatives typically contain trace amounts of lipid hydroperoxides that arise from autooxidation of the allylic chain. Typically these trace hydroperoxides are sufficient for activation of LOXs, and the subsequent product of the lipoxygenase reaction is able to activate the enzyme further. However, in some instances, at high substrate concentration, the lipid hydroperoxide product may be unable to efficiently compete with unreacted substrate for the resting, ferrous form of the enzyme, preventing autoactivation. Inclusion of exogenous lipid hydroperoxide should attenuate substrate inhibition, and such is the case for inhibition of pl12-LOX by arachidonoyltaurine. Differences in substrate affinity may account for why substrate inhibition is observed with arachidonoyltaurine but not arachidonic acid in the concentration range examined.

LOXs display distinct product profiles and specificities of oxygenation. Although 15-LOX-1 produces 15-HETE predominantly, 12-HETE accounts for 10 to 20% of total products of arachidonate oxygenation (28,55). Likewise, lk12-LOX will oxygenate arachidonate primarily at C-12 and, to a lesser extent, C-15 (56). In contrast, the regiospecifity of arachidonate oxygenation of 15-LOX-2 and pl12-LOX is more tightly controlled, with a single HETE isomer being formed almost exclusively (35,56-58). When arachidonoyltaurine was provided as substrate, both r15-LOX-1 and h15-LOX-2 generated one major product, 15-HETE-T. Similarly the mono-hydroxy product formed by lk12-LOX is predominantly 12-HETE-T, though this enzyme forms diHETE-Ts as well. Thus the fidelity of the oxygenation reaction for 15-LOX-1, 15-LOX-2 and lk12-LOX is retained, indicating that binding of the arachidonoyl chain is not significantly altered by addition of the taurine moiety.

However, pl12-LOX displays dual specificity with arachidonoyltaurine, generating both 12- and 15-HETE-T. Combined with previous studies of pl12-LOX and its substrate specificity, this provides potentially interesting implications to the model of substrate binding to pl12-LOX (23). Substrate alignment within the LOX active site is a key determinant of the product profile. As discussed above, the lipoxygenase reaction is initiated by abstraction of a *bis*-allylic hydrogen atom by the non-heme ferric iron center. The depth of the LOX substrate-binding

channel determines the position from which hydrogen is most frequently abstracted (59-61). Arachidonic acid binds to 12- and 15-LOXs in a “tail-first” orientation, with the carboxylate binding at the opening of the channel, stabilized by an ion pairing interaction (59,62), and the acyl chain extending into the hydrophobic channel. Lk12-LOX and 15-LOXs efficiently utilize neutral esters and amides of arachidonate, indicating that a hydrogen bond can substitute for the ion-pairing interaction (29-32).

The ion-pairing interaction appears to be critical for pl12-LOX, as it cannot efficiently metabolize neutral arachidonoyl species. However, pl12-LOX readily oxygenates amides of arachidonate if the substrate possesses a negatively charged headgroup, such as is present in arachidonoyltaurine and the arachidonoyl amino acids NAGly, NAla and NAGABA (23). Furthermore with these extended, negatively charged substrates, pl12-LOX acts as a 12/15-LOX. For this to occur, the substrate must adopt two different positions in the channel, one with C-10 positioned for hydrogen abstraction (to generate 12-HETE) and one that is displaced out of the channel such that C-13 is positioned above the iron center (to make 15-HETE). Thus far this phenomenon of dual specificity of pl12-LOX has only been observed with negatively charged substrates of arachidonate, suggestive of a currently unidentified determinant of substrate binding for pl12-LOX.

In order for a substrate to be metabolized *in vivo*, the compound must be able to cross membranes and reach sufficient concentrations within intracellular compartments where the potential metabolizing enzymes are located. Murine RPMs were utilized to study the cellular metabolism of arachidonoyltaurine. The eicosanoid metabolic pathways and the modulation of these pathways by inflammatory stimuli are well established in this cell line (43-50). Furthermore the lipoxygenase pathway represents a major metabolic pathway of arachidonate in unstimulated cells, although some prostaglandins are also observed. Following incubation with arachidonoyltaurine, no COX-derived products were observed, even following pre-incubation with LPS to increase COX-2 expression. This is in agreement with *in vitro* studies, which demonstrated that arachidonoyltaurine is a poor COX substrate. However, arachidonoyltaurine is rapidly taken up by RPMs and enters the lipoxygenase pathway. Arachidonoyltaurine is first oxygenated at C-12 to give rise to 12-HpETE-T. Based on the position of oxygenation and western blotting results, this reaction is most likely catalyzed by lk12-LOX. 12-HpETE-T is subsequently reduced to 12-HETE-T by a peroxidase. Biosynthesis of diHETE-T proceeds more slowly and in lower yield. Preliminary data indicate that diHETE-T is likely derived from 12-HETE-T or its parent 12-HpETE-T. However, further investigation is required to unravel the exact mechanism of diHETE-T formation.

The importance of NATs is only now beginning to be explored. This study demonstrates that a polyunsaturated NAT, arachidonoyltaurine, is metabolized by 12*S*- and 15*S*-LOXs in vitro, and is able to enter the lk12-LOX pathway in cells. LOX metabolism of arachidonoyltaurine may represent a pathway of termination or biosynthesis of signaling molecules. As the physiological role of NATs, particularly in peripheral tissues where polyunsaturated NATs are most abundant, is investigated, the role of lipid chain oxidation must also be considered.

ACKNOWLEDGMENT

We thank K. R. Kozak and J. S. Moody for the purification of h15-LO-2 and pl12-LO, respectively.

ABBREVIATIONS

FAAH, fatty acid amide hydrolase
AEA, arachidonoylethanolamide
CB1, cannabinoid receptor 1

CB2, cannabinoid receptor 2
NATs, *N*-acyltaurines
PGs, prostaglandins
HpETE, hydroperoxyeicosatetraenoic acid
HETE, hydroxyeicosatetraenoic acid
COX, cyclooxygenase
LOX, lipoxygenase
2-AG, 2-arachidonoylglycerol
NAGly, *N*-arachidonoylglycine
NAla, *N*-arachidonoylalanine
NAGABA, *N*-arachidonoyl-γ-aminobutyric acid
lk12-LOX, leukocyte-type 12*S*-LOX
pl12-LOX, platelet-type 12*S*-LOX
r15-LOX-1, rabbit reticulocyte 15*S*-LOX-1
h15-LOX-2, human 15*S*-LOX-2
oCOX-1, ovine COX-1
mCOX-2, murine COX-2
taurine, 2-aminoethane sulfonic acid
RPMs, resident peritoneal macrophages
CID, collisionally induced dissociation
13-HpODE, 13-hydroperoxyoctadecadienoic acid
HETE-T, hydroxyeicosatetraenoyltaurine
diHETE-T, dihydroxyeicosatetraenoyltaurine
LPS, bacterial lipopolysaccharide

REFERENCES

1. Pacher P, Batkai S, Kunos G. The endocannabinoid system as an emerging target of pharmacotherapy. Pharmacol. Rev 2006;58:389–462. [PubMed: 16968947]
2. Guzman M. Cannabinoids: Potential anticancer agents. Nat. Rev. Cancer 2003;3:745–755. [PubMed: 14570037]
3. Karsak M, Cohen-Solal M, Freudenberg J, Ostertag A, Morieux C, Kornak U, Essig J, Erxlebe E, Bab I, Kubisch C, de Vernejoul M-C, Zimmer A. Cannabinoid receptor type 2 gene is associated with human osteoporosis. Hum. Mol. Genet 2005;14:3389–3396. [PubMed: 16204352]
4. Kathuria S, Gaetani S, Fegley D, Valino F, Duranti A, Tontini A, Mor M, Tarzia G, la Rana G, Calignano A, Giustino A, Tattoli M, Palmery M, Cuomo V, Piomelli D. Modulation of anxiety through blockade of anandamide hydrolysis. Nat. Med 2003;9:76–81. [PubMed: 12461523]
5. Kumar R, Chambers W, Pertwee R. Pharmacological actions and therapeutic uses of cannabis and cannabinoids. Anaesthesia 2001;56:1059–1068. [PubMed: 11703238]
6. Lagneux C, Lamontagne D. Involvement of cannabinoids in the cardioprotection induced by lipopolysaccharide. Br. J. Pharmacol 2001;132:793–796. [PubMed: 11181418]
7. Ofek O, Karsak M, Leclerc N, Fogel M, Frenkel B, Wright K, Tam J, Attar-Namdar M, Kram V, Shohami E, Mechoulam R, Zimmer A, Bab I. Peripheral cannabinoid receptor, cb2, regulates bone mass. Proc. Natl. Acad. Sci. U.S.A 2006;103:696–701. [PubMed: 16407142]
8. van der Stelt M, Di Marzo V. The endocannabinoid system in the basal ganglia and in the mesolimbic reward system: Implications for neurological and psychiatric disorders. Eur. J. Pharmacol 2003;480:133–150. [PubMed: 14623357]
9. Cravatt BF, Lichtman AH. Fatty acid amide hydrolase: An emerging therapeutic target in the endocannabinoid system. Curr. Opin. Chem. Biol 2003;7:469–475. [PubMed: 12941421]
10. Saghatelian A, McKinney MK, Bandell M, Patapoutian A, Cravatt BF. A faah-regulated class of n-acyl taurines that activates trp ion channels. Biochemistry 2006;45:9007–9015. [PubMed: 16866345]

11. Saghatelian A, Trauger SA, Want EJ, Hawkins EG, Siuzdak G, Cravatt BF. Assignment of endogenous substrates to enzymes by global metabolite profiling. Biochemistry 2004;43:14332–14339. [PubMed: 15533037]
12. Kuhn H, Walther M, Kuban RJ. Mammalian arachidonate 15-lipoxygenases structure, function, and biological implications. Prostaglandins Other Lipid Mediat 2002;68-69:263–290. [PubMed: 12432923]
13. Simmons DL, Botting RM, Hla T. Cyclooxygenase isozymes: The biology of prostaglandin synthesis and inhibition. Pharmacol. Rev 2004;56:387–437. [PubMed: 15317910]
14. Yoshimoto T, Takahashi Y. Arachidonate 12-lipoxygenases. Prostaglandins Other Lipid Mediat 2002;68-69:245–262. [PubMed: 12432922]
15. Kozak KR, Marnett LJ. Oxidative metabolism of endocannabinoids. Prostaglandins Leukot. Essent. Fatty Acids 2002;66:211–220. [PubMed: 12052037]
16. Hla T, Neilson K. Human cyclooxygenase-2 cdna. Proc. Natl. Acad. Sci. U.S.A 1992;89:7384–7388. [PubMed: 1380156]
17. Percival MD, Ouellet M, Vincent CJ, Yergey JA, Kennedy BP, O'Neill GP. Purification and characterization of recombinant human cyclooxygenase-2. Arch. Biochem. Biophys 1994;315:111–118. [PubMed: 7979387]
18. Luong C, Miller A, Barnett J, Chow J, Ramesha C, Browner MF. Flexibility of the nsaid binding site in the structure of human cyclooxygenase-2. Nat. Struct. Biol 1996;3:927–933. [PubMed: 8901870]
19. Kozak KR, Prusakiewicz JJ, Rowlinson SW, Prudhomme DR, Marnett LJ. Amino acid determinants in cyclooxygenase-2 oxygenation of the endocannabinoid anandamide. Biochemistry 2003;42:9041–9049. [PubMed: 12885237]
20. Kozak KR, Prusakiewicz JJ, Rowlinson SW, Schneider C, Marnett LJ. Amino acid determinants in cyclooxygenase-2 oxygenation of the endocannabinoid 2-arachidonylglycerol. J. Biol. Chem 2001;276:30072–30077. [PubMed: 11402053]
21. Kozak KR, Rowlinson SW, Marnett LJ. Oxygenation of the endocannabinoid, 2-arachidonylglycerol, to glyceryl prostaglandins by cyclooxygenase-2. J. Biol. Chem 2000;275:33744–33749. [PubMed: 10931854]
22. Prusakiewicz JJ, Kingsley PJ, Kozak KR, Marnett LJ. Selective oxygenation of n-arachidonylglycine by cyclooxygenase-2. Biochem. Biophys. Res. Commun 2002;296:612–617. [PubMed: 12176025]
23. Prusakiewicz JJ, Turman MV, Vila A, Ball HL, Al-Mestarihi AH, Marzo VD, Marnett LJ. Oxidative metabolism of lipoamino acids and vanilloids by lipoxygenases and cyclooxygenases. Arch. Biochem. Biophys 2007;464:260–268. [PubMed: 17493578]
24. Yu M, Ives D, Ramesha CS. Synthesis of prostaglandin e2 ethanolamide from anandamide by cyclooxygenase-2. J. Biol. Chem 1997;272:21181–21186. [PubMed: 9261124]
25. Yamamoto S. "Enzymatic" Lipid peroxidation: Reactions of mammalian lipoxygenases. Free Radical Biol. Med 1991;10:149–159. [PubMed: 1901823]
26. Claeys M, Kivits GA, Christ-Hazelhof E, Nugteren DH. Metabolic profile of linoleic acid in porcine leukocytes through the lipoxygenase pathway. Biochim. Biophys. Acta 1985;837:35–51. [PubMed: 2996610]
27. Kuhn H, Sprecher H, Brash AR. On singular or dual positional specificity of lipoxygenases. The number of chiral products varies with alignment of methylene groups at the active site of the enzyme. J. Biol. Chem 1990;265:16300–16305. [PubMed: 2118902]
28. Narumiya S, Salmon JA, Cottee FH, Weatherley BC, Flower RJ. Arachidonic acid 15-lipoxygenase from rabbit peritoneal polymorphonuclear leukocytes. Partial purification and properties. J. Biol. Chem 1981;256:9583–9592. [PubMed: 6793572]
29. Edgemond WS, Hillard CJ, Falck JR, Kearn CS, Campbell WB. Human platelets and polymorphonuclear leukocytes synthesize oxygenated derivatives of arachidonylethanolamide (anandamide): Their affinities for cannabinoid receptors and pathways of inactivation. Mol. Pharmacol 1998;54:180–188. [PubMed: 9658204]
30. Kozak KR, Gupta RA, Moody JS, Ji C, Boeglin WE, DuBois RN, Brash AR, Marnett LJ. 15-lipoxygenase metabolism of 2-arachidonylglycerol. Generation of a peroxisome proliferator-activated receptor alpha agonist. J. Biol. Chem 2002;277:23278–23286. [PubMed: 11956198]

31. Moody JS, Kozak KR, Ji C, Marnett LJ. Selective oxygenation of the endocannabinoid 2-arachidonylglycerol by leukocyte-type 12-lipoxygenase. Biochemistry 2001;40:861–866. [PubMed: 11170406]
32. Ueda N, Yamamoto K, Yamamoto S, Tokunaga T, Shirakawa E, Shinkai H, Ogawa M, Sato T, Kudo I, Inoue K, Takizawa H, Nagano T, Hirobe M, Matsuki N, Saito H. Lipoxygenase-catalyzed oxygenation of arachidonylethanolamide, a cannabinoid receptor agonist. Biochim. Biophys. Acta 1995;1254:127–134. [PubMed: 7827116]
33. Kuhn H, Belkner J, Wiesner R, Brash AR. Oxygenation of biological membranes by the pure reticulocyte lipoxygenase. J. Biol. Chem 1990;265:18351–18361. [PubMed: 2120232]
34. Takahashi Y, Glasgow WC, Suzuki H, Taketani Y, Yamamoto S, Anton M, Kuhn H, Brash AR. Investigation of the oxygenation of phospholipids by the porcine leukocyte and human platelet arachidonate 12-lipoxygenases. Eur. J. Biochem 1993;218:165–171. [PubMed: 8243462]
35. Hada T, Ueda N, Takahashi Y, Yamamoto S. Catalytic properties of human platelet 12-lipoxygenase as compared with the enzymes of other origins. Biochim. Biophys. Acta 1991;1083:89–93. [PubMed: 1851637]
36. Nugteren DH. Arachidonate lipoxygenase in blood platelets. Biochim. Biophys. Acta 1975;380:299–307. [PubMed: 804329]
37. Marnett LJ, Siedlik PH, Ochs RC, Pagels WR, Das M, Honn KV, Warnock RH, Tainer BE, Eling TE. Mechanism of the stimulation of prostaglandin h synthase and prostacyclin synthase by the antithrombotic and antimetastatic agent, nafazatrom. Mol. Pharmacol 1984;26:328–335. [PubMed: 6434940]
38. Rowlinson SW, Crews BC, Lanzo CA, Marnett LJ. The binding of arachidonic acid in the cyclooxygenase active site of mouse prostaglandin endoperoxide synthase-2 (cox-2). A putative l-shaped binding conformation utilizing the top channel region. J. Biol. Chem 1999;274:23305–23310. [PubMed: 10438506]
39. Cohn ZA, Benson B. The in vitro differentiation of mononuclear phagocytes. 3. The reversibility of granule and hydrolytic enzyme formation and the turnover of granule constituents. J. Exp. Med 1965;122:455–466. [PubMed: 5320303]
40. Griffiths WJ, Yang Y, Sjovall J, Lindgren JA. Electrospray/collision-induced dissociation mass spectrometry of mono-, di- and tri-hydroxylated lipoxygenase products, including leukotrienes of the b-series and lipoxins. Rapid Commun. Mass Spectrom 1996;10:183–196. [PubMed: 8616266]
41. Murphy RC, Barkley RM, Berry K. Zemski, Hankin J, Harrison K, Johnson C, Krank J, McAnoy A, Uhlson C, Zarini S. Electrospray ionization and tandem mass spectrometry of eicosanoids. Anal. Biochem 2005;346:1–42. [PubMed: 15961057]
42. Funk MO, Isaac R, Porter NA. Preparation and purification of lipid hydroperoxides from arachidonic and g-linolenic acids. Lipids 1976;11:113–117. [PubMed: 814377]
43. Aderem AA, Cohen DS, Wright SD, Cohn ZA. Bacterial lipopolysaccharides prime macrophages for enhanced release of arachidonic acid metabolites. J. Exp. Med 1986;164:165–179. [PubMed: 2941513]
44. Bonney RJ, Opas EE, Humes JL. Lipoxygenase pathways of macrophages. Fed. Proc 1985;44:2933–2936. [PubMed: 2996948]
45. Bonney RJ, Wightman PD, Davies P, Sadowski SJ, Kuehl FA Jr. Humes JL. Regulation of prostaglandin synthesis and of the selective release of lysosomal hydrolases by mouse peritoneal macrophages. Biochem. J 1978;176:433–442. [PubMed: 743251]
46. Kurland JI, Bockman R. Prostaglandin e production by human blood monocytes and mouse peritoneal macrophages. J. Exp. Med 1978;147:952–957. [PubMed: 632752]
47. Rabinovitch H, Durand J, Gualde N, Rigaud M. Metabolism of polyunsaturated fatty acids by mouse peritoneal macrophages: The lipoxygenase metabolic pathway. Agents Actions 1981;11:580–583. [PubMed: 6803535]
48. Rouzer CA, Scott WA, Cohn ZA, Blackburn P, Manning JM. Mouse peritoneal macrophages release leukotriene c in response to a phagocytic stimulus. Proc. Natl. Acad. Sci. U.S.A 1980;77:4928–4932. [PubMed: 6933538]
49. Scott WA, Zrike JM, Hamill AL, Kempe J, Cohn ZA. Regulation of arachidonic acid metabolites in macrophages. J. Exp. Med 1980;152:324–335. [PubMed: 7400759]

50. Scott WA, Pawlowski NA, Andreach M, Cohn ZA. Resting macrophages produce distinct metabolites from exogenous arachidonic acid. J. Exp. Med 1982;155:535–547. [PubMed: 6799609]
51. Mogul R, Holman TR. Inhibition studies of soybean and human 15-lipoxygenases with long-chain alkenyl sulfate substrates. Biochemistry 2001;40:4391–4397. [PubMed: 11284695]
52. Berry H, Debat H, Larreta-Garde V. Excess substrate inhibition of soybean lipoxygenase-1 is mainly oxygen-dependent. FEBS Lett 1997;408:324–326. [PubMed: 9188786]
53. de Groot JJMC, Veldink GA, Vliegenthart JFG, Boldingh J, Wever R, van Gelder BF. Demonstration by epr spectroscopy of the functional role of iron in soybean lipoxygenase-1. Biochim. Biophys. Acta 1975;377:71–79. [PubMed: 164225]
54. Ludwig P, Holzhutter H-G, Colosimo A, Silvestrini MC, Schewe T, Rapoport SM. A kinetic model for lipoxygenases based on experimental data with the lipoxygenase of reticulocytes. Eur. J. Biochem 1987;168:325–337. [PubMed: 3117544]
55. Kilty I, Logan A, Vickers PJ. Differential characteristics of human 15-lipoxygenase isozymes and a novel splice variant of 15s-lipoxygenase. Eur. J. Biochem 1999;266:83–93. [PubMed: 10542053]
56. Burger F, Krieg P, Marks F, Furstenberger G. Positional- and stereo-selectivity of fatty acid oxygenation catalysed by mouse (12s)-lipoxygenase isoenzymes. Biochem. J 2000;348:329–335. [PubMed: 10816426]
57. Brash AR, Boeglin WE, Chang MS. Discovery of a second 15s-lipoxygenase in humans. Proc. Natl. Acad. Sci. U.S.A 1997;94:6148–6152. [PubMed: 9177185]
58. Chen XS, Brash AR, Funk CD. Purification and characterization of recombinant histidine-tagged human platelet 12-lipoxygenase expressed in a baculovirus/insect cell system. Eur. J. Biochem 1993;214:845–852. [PubMed: 8319693]
59. Gillmor SA, Villasenor A, Fletterick R, Sigal E, Browner MF. The structure of mammalian 15-lipoxygenase reveals similarity to the lipases and the determinants of substrate specificity. Nat. Struct. Biol 1997;4:1003–1009. [PubMed: 9406550]
60. Sloane DL, Leung R, Barnett J, Craik CS, Sigal E. Conversion of human 15-lipoxygenase to an efficient 12-lipoxygenase: The side-chain geometry of amino acids 417 and 418 determine positional specificity. Protein Eng 1995;8:275–282. [PubMed: 7479689]
61. Sloane DL, Leung R, Craik CS, Sigal E. A primary determinant for lipoxygenase positional specificity. Nature 1991;354:149–152. [PubMed: 1944593]
62. Gan QF, Browner MF, Sloane DL, Sigal E. Defining the arachidonic acid binding site of human 15-lipoxygenase. Molecular modeling and mutagenesis. J. Biol. Chem 1996;271:25412–25418. [PubMed: 8810309]

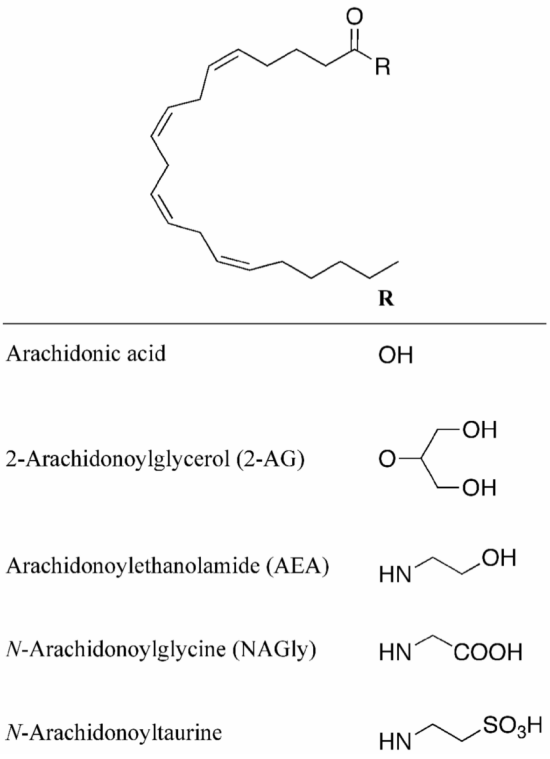

Figure 1.
Structures of arachidonoyl derivatives.

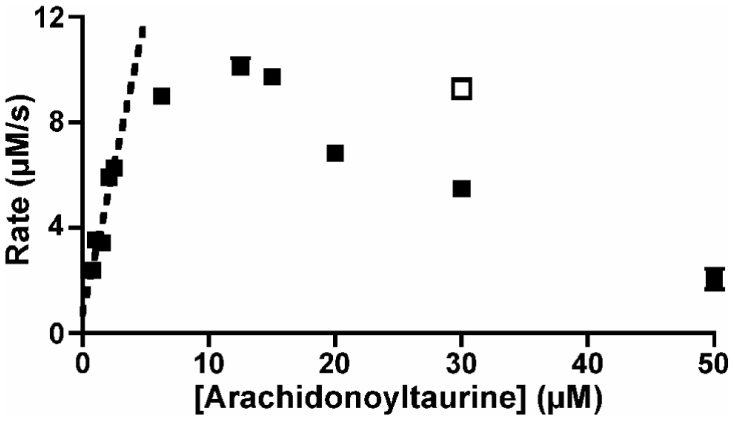

Figure 2.

Concentration-dependence of arachidonoyltaurine metabolism by pl12-LOX. Maximal rate of metabolism of arachidonoyltaurine (0.78 to 50 μM) by pl12-LOX (closed circles) was determined by monitoring change in absorbance at 236 nm. Due to substrate inhibition, data did not fit hyperbolic Michaelis-Menten equation; v_{max}/K_M was estimated from linear regression (dashed line) at low substrate concentrations. Substrate inhibition was observed at high concentrations of arachidonoyltaurine, but could be partially alleviated by co-incubation with 13-HpODE (open square). All data points represent the average ± SEM of at least two separate trials.

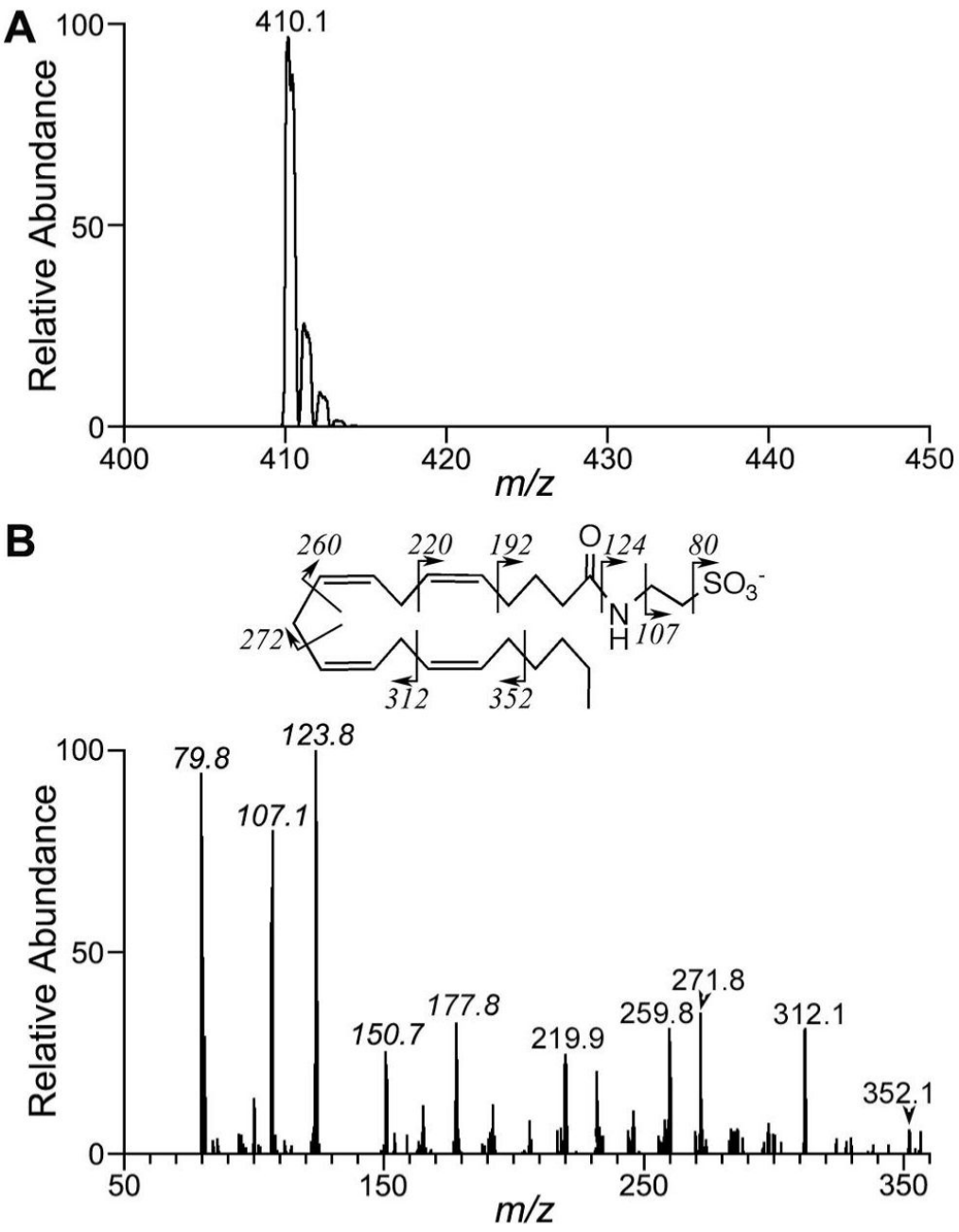

Figure 3.
MS and CID of arachidonoyltaurine in negative ion mode. *A*, Full scan MS of arachidonoyltaurine standard. *B*, CID of *m/z* 410. The structure of arachidonoyltaurine and proposed fragmentation is also shown.

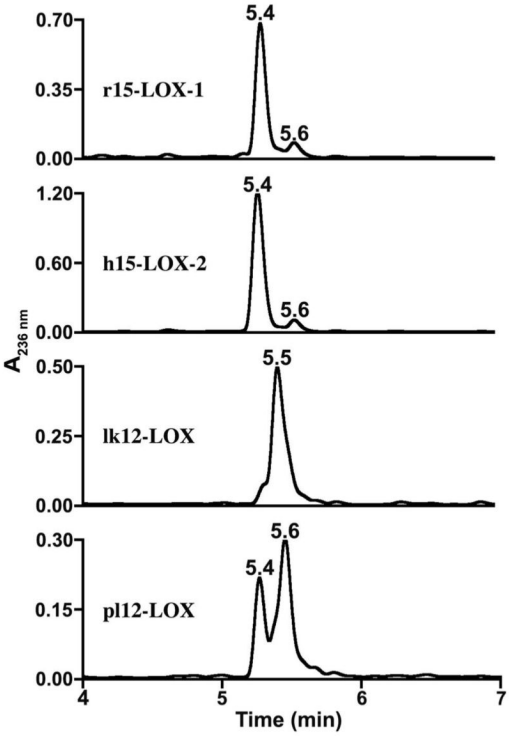

Figure 4.

UV chromatographic profiles of *in vitro* arachidonoyltaurine oxidation by LOXs. Substrate was incubated with each indicated enzyme for 15 minutes. Hydroperoxides were reduced *in situ* by addition of sodium dithionite, and products extracted and analyzed by LC-UV-MS. Chromatograms at 236 nm showed similar distribution of products as observed in the selected ion chromatograms at *m/z* 426.

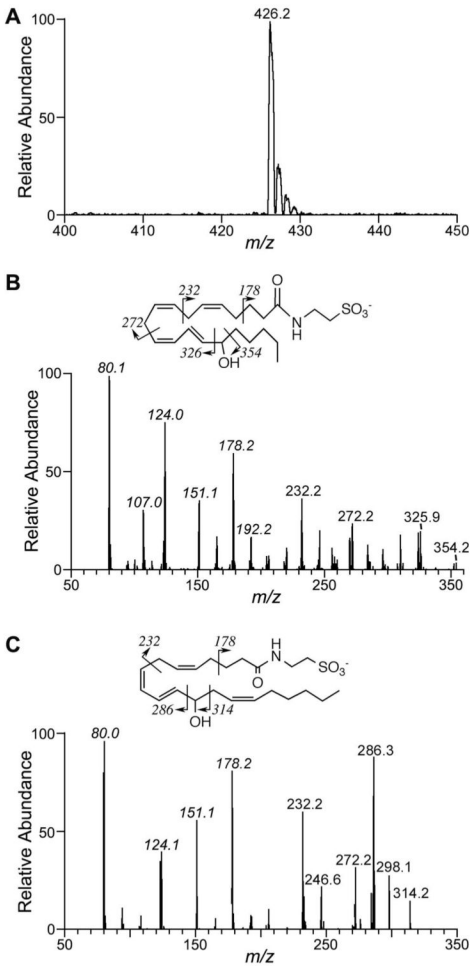

Figure 5.

MS and CID of monoxygenated products of arachidonoyltaurine metabolism in vitro. A, Full scan MS of product at 5.4 min from incubation of arachidonoyltaurine with r15-LOX-1. Products at 5.4 min and 5.6 min from enzymatic incubations afforded similar full scan MS. B, CID of product at 5.4 min. C, CID of product at 5.6 min. The proposed structure and fragmentation are also shown; ions in *italics* were also observed for arachidonoyltaurine (refer to Fig. 3).

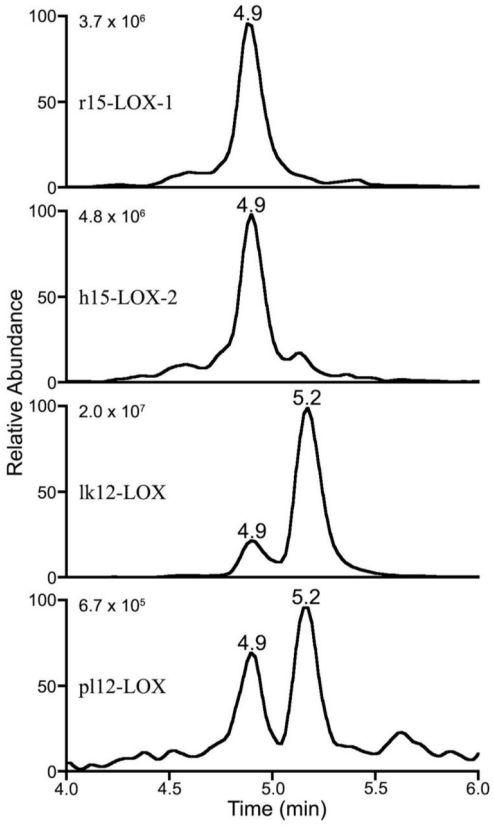

Figure 6.

Selected ion chromatograms of dioxygenated products (*m/z* 442) of *in vitro* arachidonoyltaurine oxidation by LOXs. Substrate was incubated with each indicated enzyme for 15 minutes. Hydroperoxides were reduced *in situ* by addition of sodium dithionite, and products extracted and analyzed by LC-UV-MS. The extracted chromatograms for *m/z* 442 are shown, and the absolute ion intensity is shown at the left of each panel. Absolute ion intensities for HETE-T were on the order of 3-8×10^7 for each enzyme.

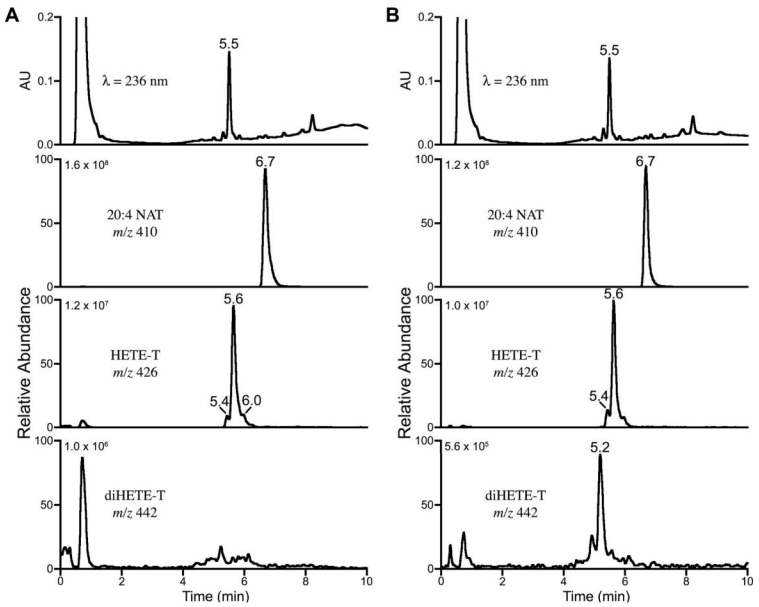

Figure 7.

Chromatographic profiles of RPMs incubated with arachidonoyltaurine. RPMs were incubated with arachidonoyltaurine for either 30 s (*A*) or 15 min (*B*). UV chromatogram at 236 nm and selected mass ranges for arachidonoyltaurine and its mono- and di-oxygenated products are shown. The absolute ion intensity is noted for each mass range.

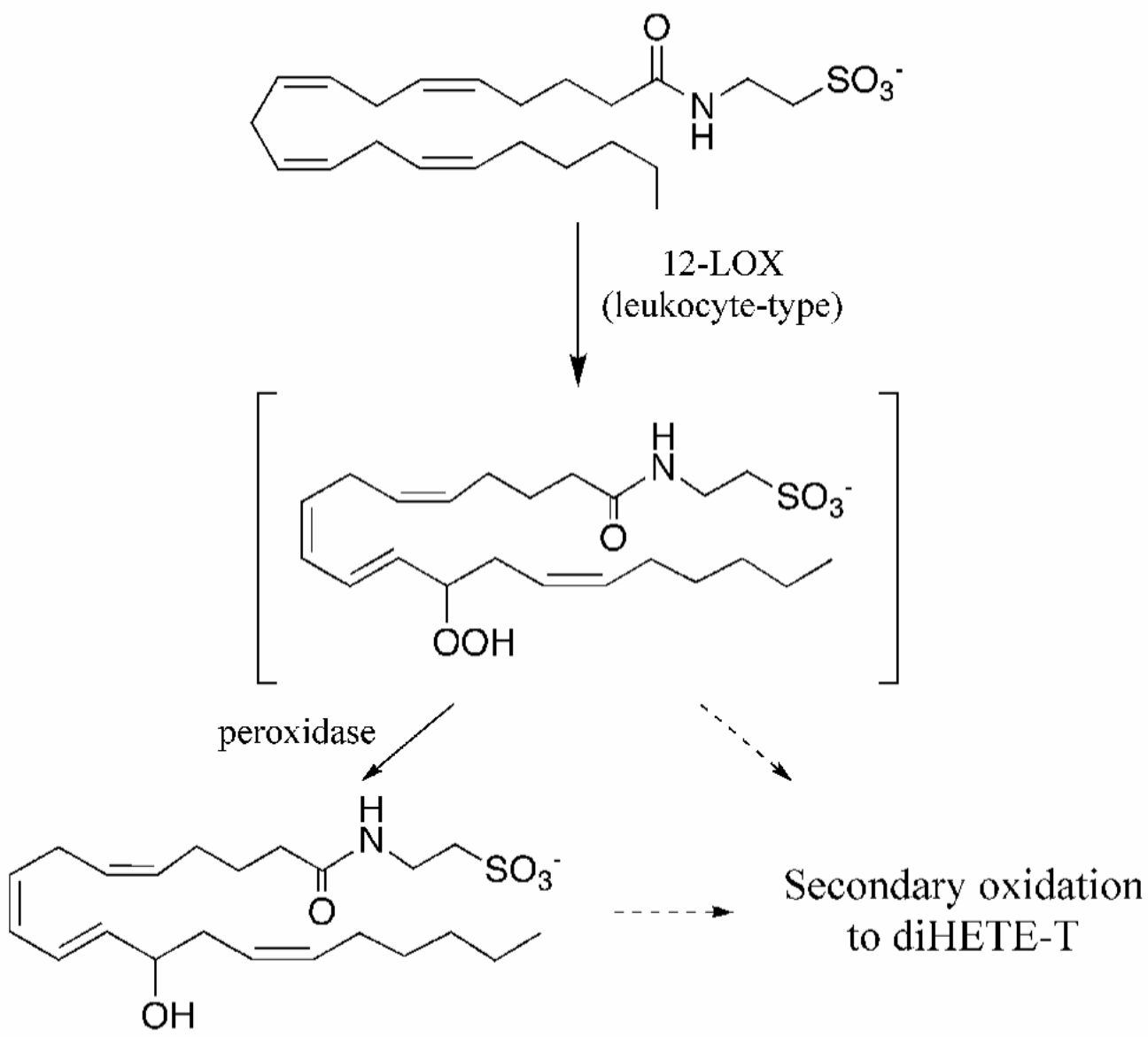

Figure 8.

Proposed pathway of arachidonoyltaurine metabolism in RPMs. Arachidonoyltaurine is rapidly converted to 12-HETE-T by a 12/15-LOX. Following prolonged incubation, a diHETE-T is observed. DiHETE-T may arise from secondary oxidation of 12-H(p)ETE-T.

Table 1

Kinetic parameters for arachidonic acid and arachidonoyltaurine metabolism by LOXs

	v_{max}/K_M(min^{-1})	
	Arachidonic acid	**Arachidonoyltaurine**
r15-LOX-1	0.45 ± 0.08[a]	0.76 ± 0.10[a]
lk12-LOX	0.38 ± 5[b]	0.41 ± 1[b]
pl12-LOX	0.36 ± 0.02[a]	2.2 ± 0.4[a]

[a] Concentration-dependence of rates could not be fit to Michaelis-Menten equation, and v_{max}/K_M ± SEM was estimated from slope of linear regression.

[b] Concentration-dependence could be fit to Michaelis-Menten equation, and v_{max}/K_M was calculated from Michaelis-Menten parameters. SEM of v_{max}/K_M was calculated from SEM of v_{max} and K_M.